American Journal of Pathology, Vol. 167, No. 3, September 2005

Growth Factors, Cytokines, Cell Cycle Molecules

Activin Controls Skin Morphogenesis and Wound Repair Predominantly via Stromal Cells and in a Concentration-Dependent Manner via Keratinocytes

Casimir Bamberger,* Agnes Schärer,* Maria Antsiferova,* Birte Tychsen,† Sandra Pankow,* Mischa Müller,* Thomas Rülicke,‡ Ralf Paus,† and Sabine Werner*

From the Department of Biology, Institute of Cell Biology, Swiss Federal Institute of Technology (ETH) Zurich, Zurich, Switzerland; the Institute of Laboratory Animal Sciences,‡ University of Zurich, Zurich, Switzerland; and the Department of Dermatology,† University Hospital Hamburg–Eppendorf, University of Hamburg, Hamburg, Germany*

The transforming growth factor-β family member activin is a potent regulator of skin morphogenesis and repair. Transgenic mice overexpressing activin in keratinocytes display epidermal hyperthickening and dermal fibrosis in normal skin and enhanced granulation tissue formation after wounding. Mice overexpressing the secreted activin antagonist follistatin, however, have the opposite wound-healing phenotype. To determine whether activin affects skin morphogenesis and repair via activation of keratinocytes and/or stromal cells, we generated transgenic mice expressing a dominant-negative activin receptor IB mutant (dnActRIB) in keratinocytes. The architecture of adult skin was unaltered in these mice, but delays were observed in postnatal pelage hair follicle morphogenesis and in the first catagen-telogen transformation of hair follicles. Although dnActRIB-transgenic mice showed slightly delayed wound re-epithelialization after skin injury, the strong inhibition of granulation tissue formation seen in follistatin-transgenic mice was not observed. Therefore, although endogenous activin appeared to affect skin morphogenesis and repair predominantly via stromal cells, overexpressed activin strongly affected the epidermis. The epidermal phenotype of activin-overexpressing mice was partially rescued by breeding these animals with dnActRIB-transgenic mice. These results demonstrate that activin affects both stromal cells and keratinocytes in normal and wounded skin and that the effect on keratinocytes is dose-dependent *in vivo*. *(Am J Pathol 2005, 167:733–747)*

Activins belong to the transforming growth factor (TGF)-β protein superfamily and were initially discovered as inducers of follicle-stimulating hormone release.[1] They determine cell fate during mesoderm induction or neurulation in *Xenopus laevis* embryos throughout a distance of several cell diameters, and thus became classical textbook morphogens.[2–4] Biologically active activins are dimeric proteins, consisting of two activin polypeptides cross-linked by a disulfide bridge.[5] Activin A (βAβA) or activin B (βBβB) are homodimers, whereas activin AB (βAβB) is a heterodimer of one activinβA and one activinβB polypeptide. The activin gene family comprises the additional, but poorly characterized members activinβC, βD, and βE.[1]

Like most members of the TGF-β family, activins mediate their biological effects through transmembrane receptor serine/threonine kinases.[6] They initially bind to a type II activin receptor (ActRII or ActRIIB) and recruit thereafter one type I activin receptor (ActRIB).[7] Receptor hetero-dimerization enables the constitutively active serine/threonine kinase of the type II receptor to phosphorylate amino acids in the GS-box present in the type I receptor. The subsequently activated serine/threonine kinase of the type I receptor phosphorylates the recruited regulatory r-Smad, Smad2, and Smad3. The latter translocate to the nucleus on multimerization with the co-Smad Smad4 and modulate as transcription factor complexes

Supported by the Deutsche Forschungsgemeinschaft (BA 2156/1-1 to C.B. and Pa 345/8-4 to R.P.), the EMBO World Programme Fellowship (WPF2004/22 to M.A.), the Swiss National Science Foundation (grant 31-61358.00 to S.W.), and the European Community/Swiss Ministry for Education and Research (to S.W).

Accepted for publication May 17, 2005.

Present address of T.R.: Institute of Laboratory Animal Science, University of Veterinary Medicine Vienna, A-1210 Vienna, Austria.

Address reprint requests to Sabine Werner, Institute of Cell Biology, HPM D42, ETH Hönggerberg, 8093 Zurich, Switzerland. E-mail: sabine.werner@cell.biol.ethz.ch.

the expression of a large variety of genes.[8] In addition to the transmembrane signaling receptors, activins bind to a secreted glycoprotein, follistatin, which sequesters activin and thus inhibits its biological activity.[9]

Among other functions, activins have been identified as regulators of skin morphogenesis. Mice deficient in the activinβA subunit lack whiskers and they have a delay in whisker follicle morphogenesis.[10] In addition, activin affects the development of interfollicular epidermis. Mice deficient in the activin antagonist follistatin display a taut shiny skin and epidermal hyperplasia, pointing to an altered balance between keratinocyte proliferation and differentiation.[11] Consistent with this finding, mice overexpressing the activinβA subunit in the basal layer of the epidermis show keratinocyte hyperproliferation and an abnormal epidermal differentiation program, including interfollicular expression of keratins 6 and 16.[12] However, keratinocyte proliferation and differentiation was not altered in the skin of mice overexpressing the secreted activin antagonist follistatin in the epidermis, indicating that the low levels of endogenous activin present in normal skin do not affect this process.[13]

In addition to skin morphogenesis, an important role of activin in wound healing has recently been demonstrated. Thus, elevated activinβA mRNA and activin A protein levels and to a lesser extent activinβB mRNA levels were found in healing mouse skin wounds.[14,15] Both activin and its antagonist follistatin can modulate the wound repair process when overexpressed in keratinocytes of transgenic mice under the control of the keratin 14 promoter. Large amounts of human activin A expressed in keratinocytes of the hyperproliferative epithelium enhanced granulation tissue formation and re-epithelialization, but also caused excessive scarring (S.W., unpublished data).[12] In contrast, mice overexpressing follistatin under the control of the same promoter had the opposite phenotype during skin wound repair.[13] Wounds of these mice displayed a thinner hyperproliferative epithelium and reduced granulation tissue formation. As one consequence, a significant reduction in wound breaking strength was observed.

Because both activin and follistatin are secreted proteins, and because activins and their receptors are expressed in different cell types of normal and wounded skin, it is as yet unclear if activin regulates skin morphogenesis and wound healing via keratinocytes or via stromal cells or both. To address this question, we expressed a serine/threonine kinase-deficient mutant of ActRIB (dnActRIB) in keratinocytes of transgenic mice. ActRIB was chosen, because it specifically binds to ActRII-activin ligand-receptor complexes[7] and because it is highly expressed in keratinocytes.[16] Thus, dnActRIB can inhibit in a dominant-negative manner activin signaling mediated by several different type I activin receptors, eg, ActRIA, ActRIB,[17] and the recently described Alk7 receptor.[18] Therefore, effects of activin on keratinocytes are inhibited, whereas the response of stromal cells to activin remains unaltered. The comparison of the phenotype of these mice with the abnormalities seen in follistatin-overexpressing mice will therefore reveal, whether endogenous activin affects skin morphogenesis and wound healing via keratinocytes or stromal cells or both. In addition, we determined if the phenotype of activin-overexpressing mice can be rescued by mating with dnActRIB mice and thus if the effect of overexpressed activin on the epidermis is direct. The results of this study show that activin affects skin morphogenesis and wound healing via keratinocytes and stromal cells in a dose-dependent manner.

Materials and Methods

Transgene Construction

The carboxy-terminally truncated murine activin receptor (ActRIB) was designed as previously described.[19] Briefly, the cDNA encoding the amino-terminal part of ActRIB, including the transmembrane domain, was amplified by polymerase chain reaction from a plasmid containing the complete murine ActRIB cDNA. The oligonucleotide hybridizing to the 3′ end of the cDNA included the coding sequences of a c-Myc epitope followed by a stop codon. The amplified cDNA fragment, designated dnActRIB, allows expression of a carboxy-terminally truncated ActRIB with an in-frame c-Myc epitope. For expression of dnActRIB in the epidermis of transgenic mice, the cDNA was completely sequenced and inserted between the intron and the poly(A) fragment of a previously described expression cassette.[12] The transgene, designated *K14-dnActRIB*, includes the following functional elements in 5′ to 3′ end order: the 2-kb human keratin 14 promoter, a 0.65-kb rabbit β-globin intron, the 0.6-kb dnActRIB cDNA, and a 0.65-kb transcription termination/polyadenylation fragment of the human growth hormone gene (Figure 1A).

Generation, Identification, and Maintenance of Transgenic Mice

Standard procedures were followed to generate transgenic mice. The 3.8-kb insert *K14-dnActRIB* was separated from vector sequences, purified, and injected into fertilized eggs obtained after superovulation of B6D2F1 females and mating with males of the same strain. Wild-type B6D2F1 mice were purchased from Elevage Janvier (Le Genest-St-Ile, France). All mice were maintained under optimal hygienic conditions and housed and fed according to federal guidelines. Mouse tail DNA was analyzed for the integration of the transgene (founder analysis) as described[13] using the rabbit β-globin intron DNA as a probe. Transgenic founders were named according to the standardized genetic nomenclature for mice as B6,D2-Tg(dnAlk4) 864-870 Zbz but in the text designated as *K14-dnActRIB* transgenic mice. The progeny was genotyped by polymerase chain reaction using oligonucleotides 5′β-globin intron (5′-gga ttc tga gaa ctt cag ggt gag-3′) and 3′β-globin intron (5′-cag cac aat aac cag cac gtt gcc-3′). These oligonucleotides hybridize to the rabbit β-globin intron in the transgene and yield a product of 621 bp in size (GB no. J00659, nucleotides 906 to 1527). Oligonucleotides hybridizing to the murine

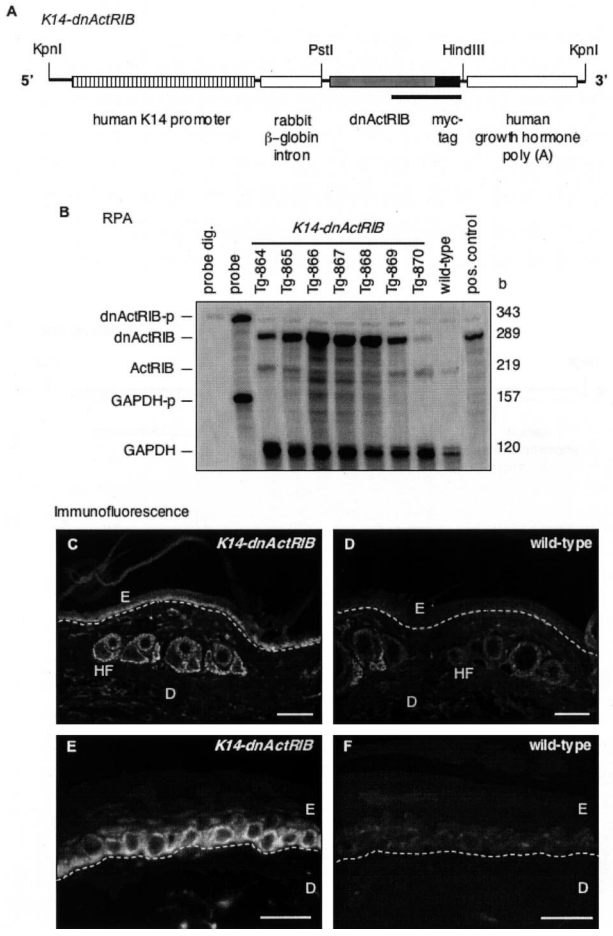

Figure 1. Generation of transgenic mice expressing a dominant-negative ActRIB mutant in the epidermis. **A:** Schematic representation of the *K14-dnActRIB* transgene. The construct includes a human keratin 14 promoter, a rabbit β-globin intron, the dnActRIB cDNA in-frame with a c-Myc epitope cDNA, and a transcription termination/polyadenylation sequence of the human growth hormone gene. The **underlined** region indicates the DNA sequence of the riboprobe used for RPA. **B:** Twenty μg of total RNA isolated from tail skin of wild-type and transgenic (*K14-dnActRIB*) mice of different lines were analyzed by RPA for the presence of endogenous ActRIB or transgene-derived dnActRIB mRNA. The same samples were additionally hybridized with a glyceraldehyde-3-phosphate dehydrogenase riboprobe (GAPDH-p) as a loading control. Ten ng of the plasmid DNA harboring the dnActRIB cDNA sequence served as a positive control. The full-length riboprobes were loaded in the lane labeled "probe" and used as a size marker. Riboprobes after digestion with RNases A and T1 were loaded in the lane labeled "probe dig." Frozen sections from tail skin of *K14-dnActRIB* transgenic (**C**, **E**) and wild-type (**D**, **F**) mice were analyzed by immunofluorescence using an antibody directed against the c-Myc epitope. A **white dotted line** indicates the location of the basement membrane. D, dermis; E, epidermis; HF, hair follicle. Scale bars: 100 μm (**C**, **D**); 50 μm (**E**, **F**).

myogenin cDNA sequence were included in each reaction tube of the genotyping polymerase chain reaction as a positive control (Mg1 5′-tta cgt cca tcg tgg aca gc-3′ and Mg2 5′-tgg gct ggg tgt tag cct ta-3′; GB no. NM_031189, nucleotides 645 to 890, fragment size: 269 bp). The following conditions were applied: 94°C for 5 minutes initial denaturation, 35 cycles of 94°C for 45 seconds, 53°C for 30 seconds, 72°C for 60 seconds, and 72°C for 5 minutes final elongation. Transgenic mice overexpressing the human HA-tagged activinβA were described previously.[12]

Wounding and Preparation of Wound Tissue

Four full-thickness excisional wounds of 0.5 cm diameter were generated on the back of wild-type and transgenic female mice (10 to 12 weeks old) by dissecting skin and panniculus carnosus as described.[20] The wounds were left untreated. Mice were sacrificed at different time points after injury. Complete wounds including 2 mm of the epidermal margins were excised. For gene expression studies, wounds from five or more mice of the same sex, age, and genotype were pooled for each individual time point investigated. Experiments were performed with at least two independent sets of pooled RNAs or protein samples for each time point. Nonwounded skin served as a negative control. All experiments with animals were performed with permission from the local veterinary authorities.

Immunohistochemistry, Histological, and Morphometrical Analysis of Sections

For histological analysis, complete wounds including 2 to 3 mm of adjacent back skin were isolated, bisected, fixed overnight in 4% paraformaldehyde/1× phosphate-buffered saline (PBS) (for histology) or in 1% acetic acid/95% ethanol (for immunofluorescence), embedded in paraffin, and cut at 6 μm thickness. Alternatively, bisected wounds or normal skin were frozen in tissue-freezing medium (Jung, Nussloch, Germany), cut at 8 μm thickness using a cryostat, and mounted on SuperFrostPlus slides (Menzel, Braunschweig, Germany).

For detection of the dnActRIB protein or keratin 6, cryosections from normal and wounded skin were dried at room temperature, rehydrated in 1× PBS for 5 minutes, fixed at 4°C with methanol/1× PBS (1:1) for 3 minutes, permeabilized with 100% methanol (−20°C) for 3 minutes, and washed in 1× PBS for 5 minutes. Pretreated cryosections or deparaffinized sections of paraffin-embedded tissues were incubated in blocking buffer and subsequently in blocking buffer containing the first antibody overnight at 4°C [polyclonal rabbit anti-c-Myc antibody, A-14 (Santa Cruz Biotechnology, Santa Cruz, CA) or polyclonal rabbit anti keratin 6 antibody (Babco, Richmond, CA)]. Bound antibodies were detected with Cy2- or Cy3-conjugated anti-rabbit IgG antibodies (Jackson Laboratories, Bar Harbor, ME), and sections were mounted in Mowiol (Sigma, Buchs, Switzerland) after a final washing step.

For histological analysis, paraffin sections were dewaxed, rehydrated, and stained with hematoxylin and eosin (H&E) according to standard procedures. For morphometrical analysis, all mounted sections were photographed using a Zeiss Axioscope2 microscope equipped with an Axiocam HRc camera (Zeiss, Jena, Germany). Morphometrical data such as the number of BrdU-positive cells, the total cell number, the length and area of the hyperthickened wound epidermis, the area of the granulation tissue, and the percentage of wound closure were obtained with the Openlab 3.1.2 software (Improvision Ltd., Basel, Switzerland). Statistical analysis

was performed using the unpaired *t*-test (Mann-Whitney test) included in the GraphPad Prism3 software package, version 3.0cx (GraphPad Software Inc., San Diego, CA). The Bonferroni correction was used for multiple comparisons. The number of wounds or skin sections is indicated by n, and N refers to the number of individual mice investigated. Only female littermates of the same age were used for direct histological comparison.

In Situ *Hybridization*

For nonradioactive *in situ* hybridization, mice were lethally anesthetized at day 5 after wounding and perfused with 0.25 mg/ml heparin (Sigma, Munich, Germany) in 1× PBS, followed by 4% paraformaldehyde/1× PBS. Complete wounds including 2 mm of adjacent uninjured tissue were isolated, bisected, frozen in tissue-freezing medium (Jung), cut at 10 μm thickness using a cryostat, and mounted on SuperFrostPlus slides (Menzel). A 609-bp DNA fragment encoding dnActRIB was used as a template for generation of digoxigenin-labeled sense (s) and anti-sense (as) riboprobes according to the protocols provided by the manufacturer (Roche, Rotkreuz, Switzerland). After pretreatment of sections,[21] hybridization was performed in a buffer containing 50% (v/v) formamide and 10 ng of digoxigenin-labeled cRNA per section at 60°C overnight. Detection of digoxigenin-labeled RNA/cRNA-hybrids with alkaline phosphatase-conjugated antibodies against digoxigenin was performed according to the recommendations of the manufacturer (Roche). The color reaction was allowed to proceed for 1 to 2 hours, stopped with 1× Tris/EDTA, and sections were mounted in Mowiol.

Detection of Proliferating Cells by Labeling with 5-Bromo-2′-Deoxyuridine (BrdU)

Mice were injected intraperitoneally with BrdU (250 mg/kg BrdU in 1× PBS; Sigma, Buchs, Switzerland) and sacrificed 2 hours after injection. Normal tail skin and bisected wounds were fixed in 4% paraformaldehyde/1× PBS overnight and embedded in paraffin. Dewaxed 6 μm sections were rehydrated, incubated with a horseradish peroxidase-conjugated monoclonal antibody directed against BrdU (Roche), and stained using 3,3′-diaminobenzidine substrate (Sigma). Counterstaining was performed with hematoxylin.

Ribonuclease Protection Assay (RPA)

For RNA preparation, excised wounds or normal back skin were immediately snap-frozen in liquid nitrogen and stored at −80°C. Isolation of total RNA and RPA were performed as described.[22,23] *In vitro* transcription of the following templates resulted in radioactively labeled riboprobes subsequently labeled with the suffix "−p". A 289-bp fragment (dnActRIB−p) corresponding to the 3′ extension coding for the c-Myc epitope and to nucleotides 347 to 564 of the murine ActRIB cDNA (GB no. NM_007395). This riboprobe allows detection of both the endogenous (219 b) and the transgene-derived (289 b) ActRIB receptor mRNA. A 155-bp fragment (activinβA−p) corresponding to nucleotides 165 to 320 of the murine activin/inhibinβA cDNA (GB no. NM_008380) and a 120-bp fragment (GAPDH−p) corresponding to nucleotides 566 to 685 of the murine glyceraldehyde-3-phosphate dehydrogenase (GAPDH) cDNA (GB no. NM_008048.1) were also used. Quantification of the results obtained by RPA was performed with the ImageQuant v1.2 software (Molecular Dynamics, Amersham, Dübendorf, Switzerland) after exposure of a storage phosphor imaging plate (Molecular Dynamics).

Culture of Primary Murine Keratinocytes

Primary murine keratinocytes were prepared and propagated as described[24] with modifications. Briefly, the epidermis of killed newborn wild-type and transgenic mice (1 to 3 days old) was separated from the dermis after Dispase II (Roche) digestion overnight. The epidermis of animals with the same genotype was pooled, and keratinocytes separated by trypsin digestion were seeded at a density of 5×10^4 cells/cm^2 in murine keratinocyte growth medium [keratinocyte serum-free medium (Invitrogen, Basel, Switzerland) supplemented with 1× penicillin/streptomycin (Invitrogen), 10^{-10} mol/L cholera toxin (Sigma), and 10 ng/ml epidermal growth factor (Sigma)]. Experiments were performed after 5 to 6 days of cell culture with change of media every second day. Keratinocyte serum-free medium (Invitrogen) containing only 1× penicillin/streptomycin was used as starvation medium.

Growth Factor Treatment, Immunocytochemistry, and Western Blot Analysis

Murine keratinocytes in primary cell culture were starved for 16 hours and subsequently stimulated with human activin A (kindly provided by Dr. D. Gospodarowicz, Chiron Corp., Emeryville, CA) or human TGF-β1 (Roche) in starvation medium for different periods of time. Cells were rinsed with 1× PBS at 4°C and lysed in lysis buffer [20 mmol/L Hepes, pH 7.5, 150 mmol/L NaCl, 10% glycerol, 1% Nonidet P-40, 10 ng/μl aprotinin, 10 ng/μl leupeptin, 10 ng/μl pepstatin, 500 nmol/L 4-(2-aminoethyl)-benzenesulfonyl fluoride, 1 mmol/L ethylenedinitrilo-tetraacetic acid, 1 mmol/L sodium vanadate, 100 μmol/L phenylarsine oxide, 50 mmol/L sodium fluoride, 10 mmol/L sodium pyrophosphate, 40 mmol/L β-glycerophosphate]. The total cell lysate was sonicated and centrifuged for 15 minutes at 4°C in a microcentrifuge. Total cell lysates were mixed with Laemmli sample buffer, incubated for 5 minutes at 95°C, and analyzed by denaturing 10% polyacrylamide gel electrophoresis, followed by Western blotting. Membranes were incubated with a polyclonal rabbit antibody directed against phosphorylated Smad2 (kindly provided by Dr. C.H. Heldin, Ludwig Institute for Cancer Research, Uppsala, Sweden and Dr. P. ten Dijke, The

Netherlands Cancer Institute, Amsterdam, The Netherlands) or with a monoclonal antibody directed against the c-Myc epitope (Santa Cruz), with a rabbit polyclonal antibody detecting Smad2 and Smad3 (FL-425, Santa Cruz), or with a monoclonal antibody directed against cytoplasmic β-actin (AC-15, Sigma). Bound horseradish peroxidase-coupled secondary antibodies (Promega, Madison, WI) were detected with the ECL (Amersham, Dübendorf, Switzerland) or the SuperSignal West Femto maximum sensitivity substrate (Pierce, Lausanne, Switzerland) detection systems. Signal intensities on exposed X-ray films were quantified with NIHimage software (NIH, Bethesda, MD). Background-corrected intensities of phosphorylated Smad2 signals were normalized to β-actin signals.

For immunocytochemistry, cultured murine keratinocytes were fixed in 4% paraformaldehyde, followed by methanol/1× PBS (1:1) and permeabilized with 100% methanol (−20°C). Blocking was performed with blocking solution (10% horse serum, 0.5% bovine serum albumin, 1× PBS) at room temperature for 1 hour and cells were incubated with goat polyclonal anti-Smad2/3 antibody (E-20, Santa Cruz) or with rabbit polyclonal anti c-Myc epitope antibody (A-14, Santa Cruz) in blocking solution overnight at 4°C. Cy3-conjugated anti-rabbit IgG or anti-goat IgG antibodies (Jackson Laboratories) were used to detect bound primary antibodies. Sections were mounted in Mowiol.

Histomorphometry of Hair Follicles

One percent acetic acid/ninety-five percent ethanol-fixed and paraffin-embedded murine back skin was cut in sections of 5 μm thickness and stained with hemalaun and eosin. The stage of pelage hair follicles was evaluated in the skin of *K14-dnActRIB* transgenic and wild-type mice during morphogenesis and during the first hair cycle according to published criteria.[25,26] At least 20 hair follicles from four different wild-type or transgenic mice each were examined by light microscopy. Cell proliferation was assessed by immunofluorescence for the proliferation-associated Ki67 protein complex. Peroxidase-coupled secondary antibodies (Jackson Laboratories) bound to murine monoclonal anti-Ki67 antibodies (Dianova, GmbH, Hamburg, Germany) were visualized using 3,3-diaminobenzidine-tetrachloride as a chromogen as previously described.[27] All Ki67-positive cells below the Auber's line as well as the total number of keratinocytes were counted. The amount of Ki67-positive cells was given in percent.

Results

K14-dnActRIB *Transgenic Mice Express High Levels of the Transgene in Keratinocytes of the Skin*

A dominant-negative mutant of the activin receptor IB with an in-frame c-Myc tag was expressed in the epidermis of transgenic mice under the control of a human keratin 14 promoter (Figure 1A).[12] Before the generation of *K14-dnActRIB* transgenic mice, expression of the dnActRIB protein from the transgene was verified in transient transfection experiments of COS-1 and HaCaT cells (not shown). Transgenic founder mice gave rise to seven independent *K14-dnActRIB* transgenic mouse lines in a B6,D2 mixed background (line 864-870). RPA visualized dnActRIB mRNA in total RNA preparations from the tail tips of mice from these lines (Figure 1B). The riboprobe dnActRIB-p (indicated as a black bar in Figure 1A) detects simultaneously endogenous ActRIB (219 b) and transgene-derived dnActRIB (289 b) mRNAs. When compared to endogenous ActRIB mRNA, the extent of dnActRIB mRNA overexpression ranged from 0.5× (Tg-870) to 14× (Tg-866). This extent of overexpression is most likely underestimated, because the endogenous receptor is expressed in many different cell types, whereas the transgene is only expressed in basal keratinocytes and hair follicle keratinocytes. Further analysis focused on mouse line Tg-868 with a 12× overexpression of the dnActRIB mRNA unless otherwise indicated. Line Tg-866 (14× overexpression) and line Tg-865 (6× overexpression) were used to confirm some of the results obtained with line Tg-868. Immunohistochemistry with a monoclonal antibody directed against the c-Myc tag revealed the presence of dnActRIB-positive keratinocytes in the basal layer of the epidermis, hair follicles, and sebaceous glands in *K14-dnActRIB* transgenic mice (Figure 1, C and E). A weak staining observed in tail skin sections of wild-type mice most likely results from antibody binding to the endogenous c-Myc protein (Figure 1, D and F).

Activin A-Mediated Signal Transduction Is Inhibited in Cultured Keratinocytes from K14-dnActRIB *Transgenic Mice*

High levels of dnActRIB transcripts were present in cultured primary keratinocytes from transgenic mice, whereas only endogenous ActRIB mRNA was found by RPA in keratinocytes from wild-type mice (Figure 2A). Quantification of the RPA signals revealed an overexpression of dnActRIB compared to ActRIB of more than a factor of 25 after normalization to GAPDH levels. Moreover, Western blotting of protein lysates from cultured keratinocytes revealed the presence of two dnActRIB protein variants of ~22 kd and 27 kd in keratinocytes from transgenic mice. These two variants may result from different glycosylation of the precursor protein (Figure 2B). In addition, keratinocytes from *K14-dnActRIB* transgenic mice expressed high levels of dnActRIB protein as visualized by immunofluorescence (Figure 2C). A particularly strong staining was observed around the nuclei, indicating its translation at the endoplasmatic reticulum and transport via the Golgi apparatus. A different staining pattern at lower signal intensity was seen in keratinocytes from wild-

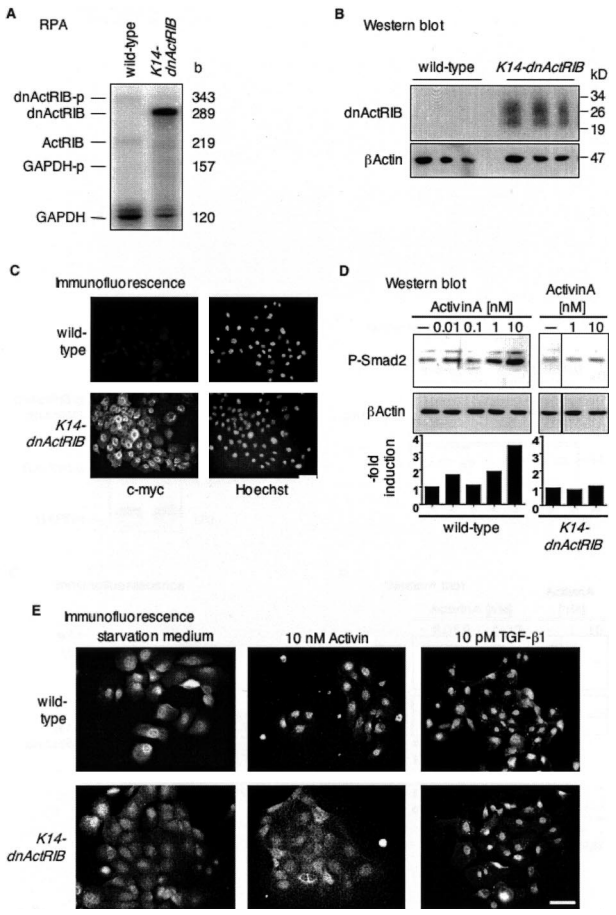

Figure 2. Inhibition of activin receptor signaling in primary keratinocytes from *K14-dnActRIB* transgenic mice. **A:** Five μg of total RNA isolated from cultured murine keratinocytes were analyzed for the expression of the endogenous ActRIB and transgene-derived dnActRIB mRNA by RPA. **B:** Western blotting of 20 μg of protein of different cell lysates from keratinocytes of wild-type and transgenic mice was performed to identify the dnActRIB protein. The membrane was incubated with a monoclonal antibody directed against the c-Myc epitope and reprobed with an antibody directed against β-actin as a loading control. **C:** Cultured primary murine keratinocytes were analyzed for the presence of the dnActRIB protein. After fixation and permeabilization, the c-Myc tag was detected with an antibody directed against c-Myc, and nuclei were visualized with Hoechst 33258. After a 24-hour starvation period, murine keratinocytes in primary cell culture were treated for 60 minutes (**D**) or 2.5 hours (**E**) with different concentrations of human activin A or TGF-β1 as indicated. **D:** Phosphorylated Smad2 proteins were detected by Western blotting. The membrane was reprobed with an antibody directed against cytoplasmic β-actin as a loading control. The induction in the levels of phosphorylated Smad2 relative to control is represented in a bar graph below the blot. The amount of phosphorylated Smad2 was normalized to β-actin at each individual time point. **E:** Activin A- or TGF-β1-mediated nuclear translocation of Smad2/3 was monitored in murine keratinocytes from *K14-dnActRIB* or wild-type mice by immunofluorescence using a polyclonal antibody directed against Smad2/3. Scale bar, 50 μm.

type mice and most likely reflects the recognition of endogenous c-Myc protein by the antibody.

dnActRIB has been described to inhibit activin-mediated phosphorylation of r-Smads.[19] To verify this effect in *K14-dnActRIB* transgenic mice, murine keratinocytes kept in primary cell culture were stimulated for 2 hours with human activin A, and phosphorylated Smad2 proteins were subsequently detected by Western blotting (Figure 2D). dnActRIB blocked Smad2 phosphorylation, which was observed at high concentrations of activin A in keratinocytes from wild-type mice. By contrast, TGF-β1-mediated Smad2 phosphorylation was not affected (data not shown).

Receptor-mediated phosphorylation of r-Smad results in nuclear accumulation of Smad protein complexes.[6,16] Immunocytochemistry revealed that after 4 hours of stimulation with activin A, the translocation of Smad2/3 proteins into the nucleus was strongly reduced in keratinocytes from *K14-dnActRIB* transgenic animals (Figure 2E). These results show that the activin A signaling pathway is inhibited by dnActRIB in murine keratinocytes. By contrast, the nuclear translocation of Smad2/3 after stimulation with TGF-β1 was unaltered in *K14-dnActRIB* keratinocytes, further suggesting that TGF-β-mediated signaling is not affected.

Adult K14-dnActRIB *Transgenic Mice Lack Obvious Skin Abnormalities*

K14-dnActRIB transgenic mice displayed no macroscopically visible differences in comparison to their wild-type littermates at birth, during weaning, and in adulthood. In contrast to follistatin-overexpressing mice, which are born with opened eyelids,[13] the eyelids of *K14-dnActRIB* transgenic mice were closed at birth. Furthermore, all extremities were fully developed. Histological examination of the tail and back skin of adult mice revealed no overt difference in the architecture of the epidermis, dermis, and appendages. Consistent with the lack of histological abnormalities, keratinocyte differentiation was not altered as determined by immunostaining with antibodies against keratins 14, 10, and 6 (data not shown and Figure 6). Likewise, the distribution of the basal lamina proteins collagen IV and laminin-1 was identical (not shown).

The proliferation rate of keratinocytes in the interfollicular epidermis was determined by BrdU incorporation. The number of BrdU-labeled cells ($BrdU^+$) per mm basement membrane in tail skin of transgenic mice was comparable to wild-type mice independent of the genetic background (B6,D2 mixed background or CD1/B6,D2 mixed background) (Figure 3A and Figure 7C). In addition, the proliferation rate was similar in back skin epidermis from wild-type and *K14-dnActRIB* transgenic mice in a B6,D2 background (Figure 3B).

K14-dnActRIB *Transgenic Mice Show Discrete Abnormalities in Hair Follicle Development and in the Initiation of Hair Follicle Cycling*

K14-dnActRIB transgenic mice showed no overt morphological abnormalities in hair shaft formation and in hair follicle development or cycling. However, quantitative histomorphometry revealed subtle abnormalities during hair follicle development and cycling: compared to wild-type controls, mice with defective activin receptor signaling showed a slight, yet significant retardation of hair follicle morphogenesis. One day after birth ~60% of the hair follicles were in early morphogenesis stages (stages

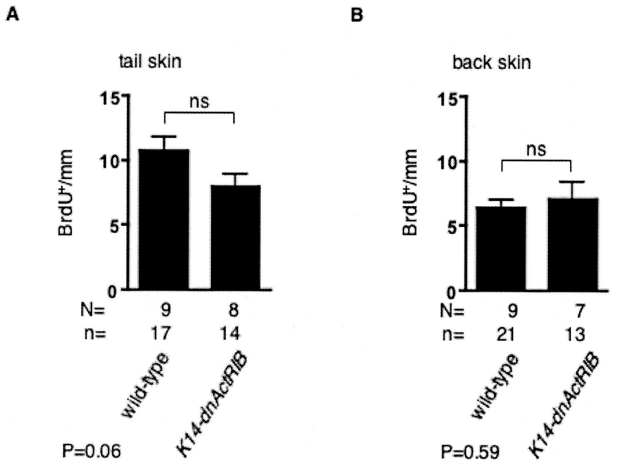

Figure 3. Unaltered keratinocyte proliferation in the skin of *K14-dnActRIB* transgenic mice. The number of BrdU-positive keratinocytes in tail skin (**A**) or back skin (**B**) of *K14-dnAcRIB* transgenic and wild-type mice with a B6,D2 mixed background was determined per mm length of basement membrane. Error bars indicate SEM. The significance between two groups was determined by Student's *t*-test. The determined *P* value is given below the corresponding bar graph. n, number of skin sections; N, number of animals.

1 and 2 on an 8-stage scale, according to the criteria described by Paus and colleagues[25] and Schmidt-Ullrich and Paus[28]), and 30% of the hair follicles were in mid morphogenesis stages 3 to 5 (Figure 4A). In control animals, ~45% were in early stages of hair follicle development, whereas 50% of hair follicles had already reached stages 3 to 5 one day after birth.

At the end of hair follicle morphogenesis (around P17), hair follicle cycling is initiated by entry into the first stage of apoptosis-driven hair follicle regression (catagen).[26,29,30] According to the previously published criteria for hair cycle-stage classification,[26] a slight, but significant delay in the first spontaneous catagen-telogen transformation was seen in transgenic mice: 17 days p.p., almost 90% of the follicles in transgenic mice were still in the early and middle stages of catagen development, whereas mid and late stages of catagen development predominated in wild-type mice, in which more than 10% of the hair follicles had even entered into telogen already (Figure 4B).

This discrete delay of the catagen-telogen transformation in *K14-dnActRIB* transgenic mice was independently corroborated by the demonstration that transgenic hair bulbs displayed a significantly higher percentage of keratinocytes that were still proliferating (eg, number of $Ki67^+$ cells below Auber's line, ie, in the most proliferation-intensive hair follicle compartment) (Figure 4C). No difference in pelage hair follicle cycling and morphology was observed between *K14-dnActRIB* transgenic and wild-type mice at day 25 p.p., ie, when murine pelage hair follicles normally all have entered into their first stage of relative quiescence (telogen).[26,29] These findings indicate that normal activin signaling in keratinocytes affects hair follicle keratinocytes in a manner that promotes progression of early stages of both hair follicle morphogenesis and the first catagen-telogen transformation during the onset of hair follicle cycling.

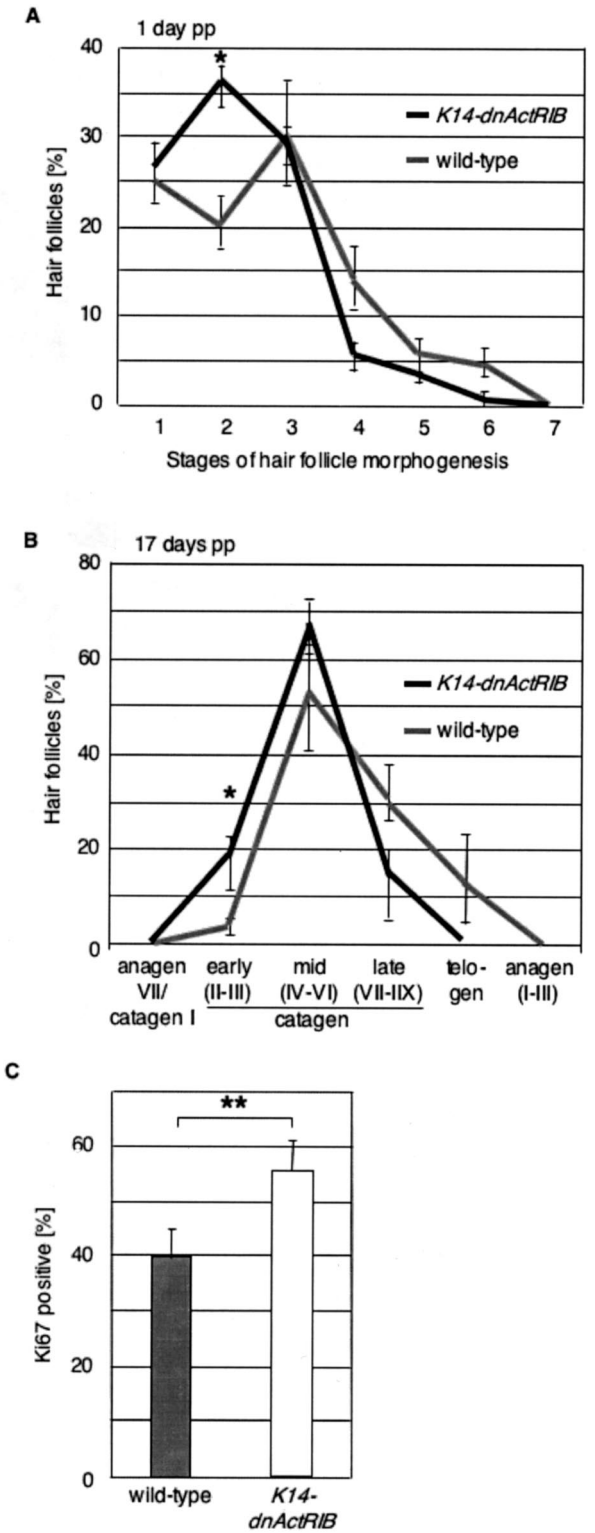

Figure 4. Delayed hair follicle morphogenesis in *K14-dnActRIB* transgenic mice. **A:** Pelage hair follicles in the back skin of *K14-dnActRIB* transgenic and wild-type mice 1 day after birth were evaluated according to the hair follicle morphogenesis stages defined in Paus and colleagues.[25] Higher values indicate later stages in the hair cycle, $*P = 0.018$. **B:** Pelage hair follicles were categorized at the end of the first hair cycle at day 17 pp. **C:** The percentage of Ki67-positive cells underneath the Auber's line in pelage hair follicles was determined at day 17 pp. Error bars indicate standard errors of mean. The significance of the difference between wild-type and transgenic mice was determined by Student's *t*-test. $*P < 0.05$, $**P < 0.01$; *P* values determined with analysis of variance test.

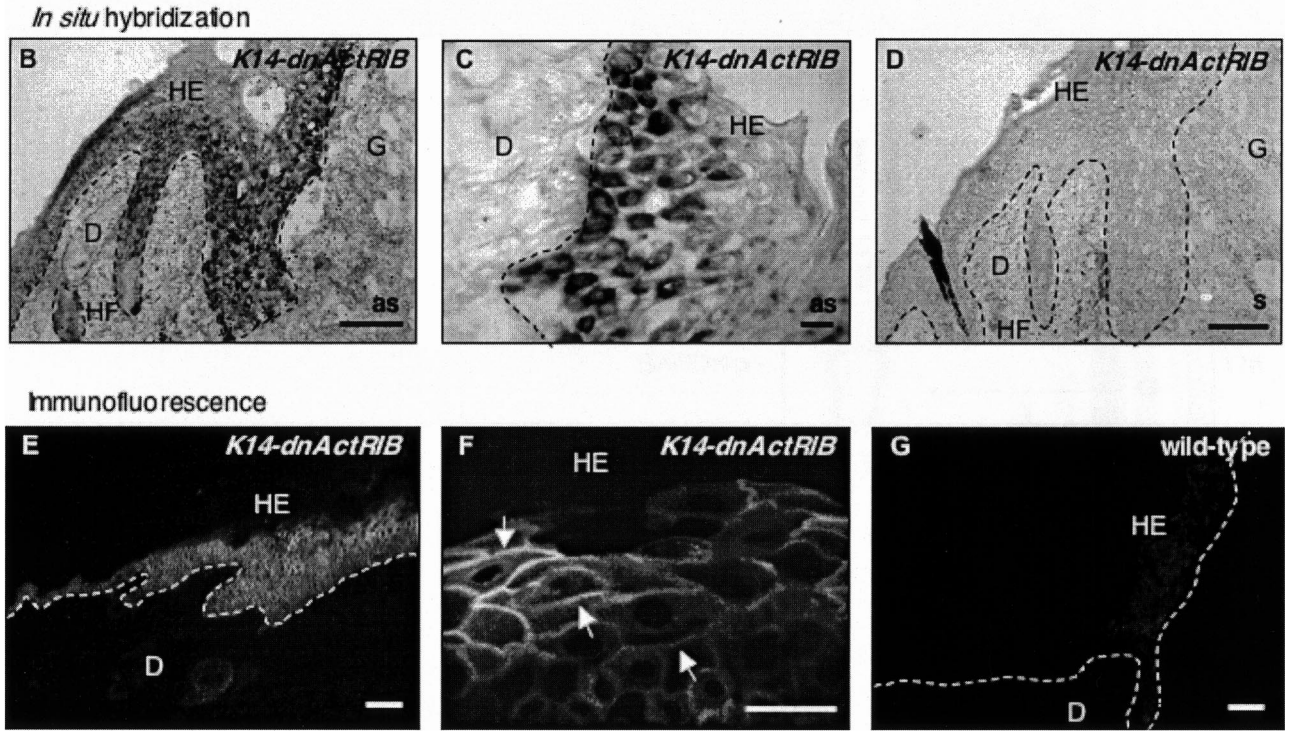

Figure 5. dnActRIB is highly expressed in full-thickness skin wounds. **A:** Twenty-μg samples of total cellular RNA from normal and wounded skin of different stages from wild-type mice and transgenic animals (line Tg-868) were analyzed for the presence of dnActRIB mRNA by RPA. Hybridization with a GAPDH riboprobe served as a loading control. A low amount of the riboprobes was loaded in the lane labeled "probes" and used as a size marker. Riboprobes digested with RNases A and T1 were loaded in the lane labeled "probes dig." **B–D:** Frozen sections from day 5 wounds of *K14-dnActRIB* transgenic mice were analyzed by nonradioactive *in situ* hybridization for the presence of dnActRIB mRNA. An overview over one half of a wound is shown in **B**. Note the strong expression of the transgene in basal and suprabasal layers of the hyperproliferative epithelium. A higher magnification of an independent section is shown in **C**. **D:** A section adjacent to the one shown in **B** was hybridized with the sense riboprobe. **E–G:** Cryosections of day 5 wounds from *K14-dnActRIB* transgenic (**E**, **F**) and wild-type (**G**) mice were analyzed by immunofluorescence using an antibody directed against the c-Myc epitope. A strong signal was detected in basal and suprabasal keratinocytes of the wound epidermis of *K14-dnActRIB* transgenic mice. A higher magnification (**F**, **arrows**) revealed membrane-associated localization of dnActRIB. The weak staining observed in wound epidermis of wild-type mice most likely results from the endogenous c-Myc protein. as, anti-sense; D, dermis; HE, hyperproliferative wound epidermis; HF, hair follicle; G, granulation tissue; s, sense. Scale bars: 100 μm (**B**, **D**, **E**, **G**); 50 μm (**C**, **F**).

Hyperproliferative Keratinocytes at the Rim of Skin Wounds Express High Levels of dnActRIB

To investigate the influence of endogenous activin on keratinocytes during normal skin wound repair, full-thickness excisional wounds were generated on the backs of *K14-dnActRIB* transgenic mice and wild-type littermates. Consistent with the up-regulation of keratin 14-driven transgene expression during skin wound healing,[12,13] dnActRIB mRNA expression in day 5 wounds was induced up to threefold when normalized to GAPDH mRNA levels and compared to normal back skin (Figure 5A). Nonradioactive *in situ* hybridization localized dnActRIB mRNA in the hyperproliferative epithelium of day 5 wounds (Figure 5B). Higher magnifications of the hyperproliferative epithelium revealed strong expression of the transgene in basal and some suprabasal keratinocytes (Figure 5C). Control hybridization with the corresponding dnActRIB sense riboprobe on adjacent sections showed only unspecific staining (Figure 5D). Cryosections of day 5 wounds of wild-type mice incubated with the dnActRIB anti-sense riboprobe showed a very faint signal in the normal epidermis and in the hyperproliferative wound epithelium, most likely resulting from the detection of endogenous ActRIB mRNA (not shown).

Immunofluorescence detected the dnActRIB protein in the hyperproliferative epithelium of day 5 skin wounds from *K14-dnActRIB* transgenic mice (Figure 5E). The dnActRIB protein was found in almost all keratinocytes of the hyperproliferative epithelium. A higher magnification of an independent section shows that the dnActRIB protein is localized at the membrane of keratinocytes (Figure 5F, arrows). Sections of wild-type mice displayed a weak and homogenous staining of the cytoplasm of hyperproliferative keratinocytes, which may reflect the presence of endogenous c-Myc protein (Figure 5G).

Delayed Re-Epithelialization in K14-dnActRIB *Transgenic Mice*

After injury, keratinocytes at the wound rim hyperproliferate to cover the wounded area. Histological examination of H&E-stained transverse sections from the middle of

wounds at days 3 and 5 after injury revealed no difference in the gross morphology of the wounds between wild-type and *K14-dnActRIB* transgenic mice (Figure 6A). Thirteen days after wounding, the wound was completely covered by keratinocytes, and tissue remodeling in the injured area was not obviously altered. RPA showed normal up-regulation of activinβA mRNA during wound repair in both *K14-dnActRIB* transgenic and wild-type mice throughout the healing process (Figure 6B), consistent with previously published data.[14] In addition, the mRNA levels of the activin antagonist follistatin were equally low and unaltered in wounds of transgenic and wild-type mice, and the mRNA expression levels of collagenα1(I), collagenα1(III), and fibronectin were equal in mice of both genotypes (not shown).

The distribution of several keratinocyte differentiation marker proteins (keratins 14, 10, and 6) was not obviously altered in wounds of *K14-dnActRIB* transgenic mice when compared to wild-type mice. Equal expression patterns were also observed for the basal lamina proteins collagen IV, laminin-1, and tenascin-C (data not shown). Interestingly, the percentage of fully re-epithelialized wounds at day 5 after injury was much lower in *K14-dnActRIB* transgenic mice (49%) compared to control animals (75%) (Figure 6C). To determine whether the reduced wound closure is due to reduced wound contraction or reduced re-epithelialization, we first measured the distance between both wound edges. However, no significant difference was observed between wild-type and transgenic mice (data not shown), indicating that the difference in wound closure results from alterations in re-epithelialization. The latter can be due to reduced proliferation, enhanced apoptosis, or reduced migration. BrdU-incorporation assays were performed to investigate the influence of dnActRIB expression on cell proliferation. Despite the slightly delayed wound closure, keratinocytes in the hyperproliferative epithelium of *K14-dnActRIB* transgenic mice displayed unaltered BrdU incorporation rates when compared to wild-type mice (Figure 6D). Therefore, the reduced re-epithelialization is not due to reduced keratinocyte proliferation. Consistent with this finding, the area of the neo-epidermis was unaltered in transgenic mice (Figure 6E). Furthermore, the number of apoptotic cells in the hyperproliferative epidermis was equally low in mice of both genotypes as determined by terminal-deoxynucleotidyl transferase-mediated dUTP nick labeling (TUNEL) assays (data not shown). Therefore, the difference in re-epithelialization is probably a result of reduced movement of keratinocytes at the wound rim. Supporting this hypothesis, the length of the wound epidermis was shorter in *K14-dnActRIB* transgenic mice (Figure 6F).

The Epidermal Phenotype Resulting from ActivinβA Overexpression in Keratinocytes Is Partially Rescued in Mice Double Transgenic for K14-dnActRIB and K14-ActivinβA

The strongly delayed wound healing, in particular the defect in granulation tissue formation, which we observed in *K14-follistatin* transgenic mice, was not recapitulated in *K14-dnActRIB* transgenic mice, indicating that keratinocytes are not the major target of endogenous activin in the wound. Because activin is known to be a morphogen and thus exerts dose-dependent effects, we wondered if enhanced levels of activin directly affect the epidermis. To test this possibility, we mated transgenic mice, which overexpress activinβA under the human keratin 14 promoter in the epidermis (*K14-activinβA*),[12] with *K14-dnActRIB* transgenic mice (this study). Interestingly, the reduced tail length of activinβA-overexpressing mice, which results from epidermal hyperkeratosis and necrosis at the tail tip (unpublished data),[12] was partially rescued in *K14-dnActRIB/K14-activinβA* double-transgenic animals (Figure 7), demonstrating that this phenotype is at least partially mediated via activin action on keratinocytes. Consistent with this observation, the epidermal hyperthickening of activinβA-overexpressing mice was partially rescued by breeding of the animals with *K14-dnActRIB* transgenic mice (Figure 7B). Furthermore, keratinocyte proliferation as determined by BrdU incorporation returned to almost normal levels in double-transgenic mice, and was comparable to the proliferation rate observed in *K14-dnActRIB* single-transgenic and wild-type mice (Figure 7C).

As revealed by high-magnification photographs of the tail skin, *K14-activinβA* transgenic mice have densely packed keratinocytes in the basal layer and an irregular border between the dermis and the epidermis. Again, this phenotype was rescued in *K14-dnActRIB/K14-activinβA* double-transgenic mice (Figure 7D). Finally, a strong interfollicular expression of keratin 6 was observed in *K14-activinβA* transgenic mice (Figure 7D).[12] *K14-dnActRIB/K14-activinβA* mice showed only a weak and patchy expression of keratin 6 in the epidermis, and this keratin was completely absent in interfollicular epidermis of wild-type and *K14-dnActRIB* single-transgenic mice. These results demonstrate that pathologically high activin levels in the epidermis can directly influence epidermal thickness, keratinocyte proliferation, and differentiation via activin receptor-mediated signaling in keratinocytes.

Overexpression of activin in keratinocytes not only influences the architecture of the epidermis but also results in replacement of subdermal fatty tissue by connective tissue (Figure 7E).[12] As expected, this phenotype was observed in mice overexpressing both activinβA and dnActRIB, indicating that the high levels of activin produced in the epidermis diffuse into the underlying dermis. As a diffusible morphogen, activin can influence the underlying dermis in *K14-dnActRIB/K14-activinβA* double-transgenic mice despite the overexpression of dnActRIB in keratinocytes.

Discussion

Recent studies revealed an important role of the growth and differentiation factor activin in cutaneous wound repair.[31] Thus, overexpression of the soluble activin antagonist follistatin in the epidermis of transgenic mice caused a strong delay in granulation tissue formation and

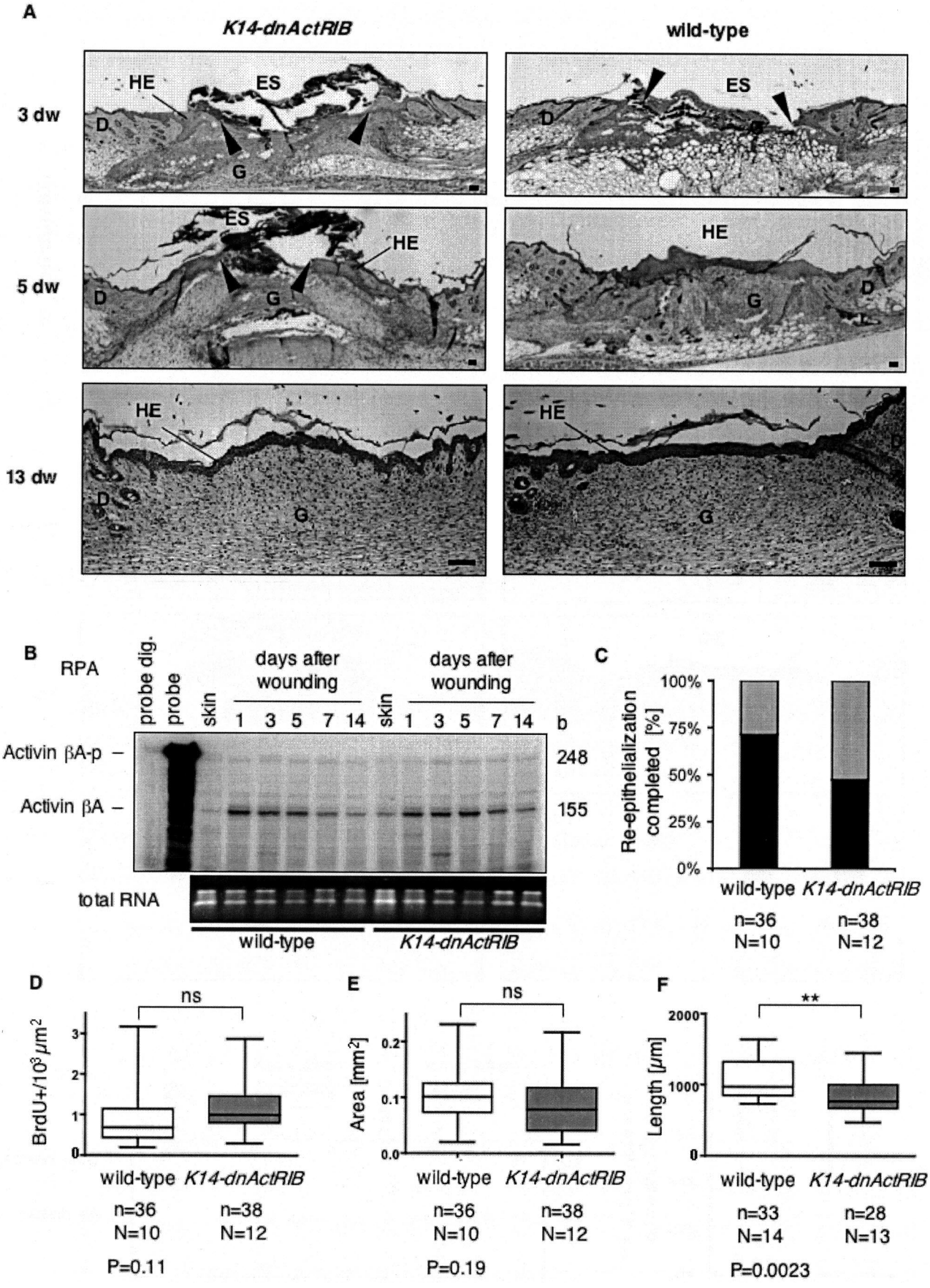
A
K14-dnActRIB
wild-type
3 dw
5 dw
13 dw
HE
ES
D
G
B
RPA
probe dig.
probe
skin
days after wounding
1 3 5 7 14
b
Activin βA-p
Activin βA
248
155
total RNA
wild-type
K14-dnActRIB
C
Re-epithelialization completed [%]
100%
75%
50%
25%
0%
wild-type
K14-dnActRIB
n=36
N=10
n=38
N=12
D
BrdU+/10³ μm²
ns
n=36
N=10
n=38
N=12
P=0.11
E
Area [mm²]
ns
P=0.19
F
Length [μm]
2000
1000
0
**
n=33
N=14
n=28
N=13
P=0.0023

wound re-epithelialization, demonstrating a crucial function of endogenous activin in these processes.[13] Consistent with this finding, overexpression of activin in the epidermis of transgenic mice enhanced the process of wound repair.[12] In addition, the overexpressed activin also affected skin morphogenesis as demonstrated by the dermal fibrosis and epidermal hyperplasia, which were observed in these animals.[12] Because both activin and follistatin are secreted proteins and because activin receptors are present on stromal cells and keratinocytes,[31] activin may regulate skin morphogenesis and wound healing via keratinocytes or stromal cells or both. To distinguish between these possibilities, we generated transgenic mice with disrupted activin receptor signaling in keratinocytes. This strategy allowed us to determine whether endogenous and overexpressed activin directly affect this cell type in normal and wounded skin. In addition, effects of activin on stromal cells will be revealed by comparison of the phenotype in *K14-dnActRIB* transgenic mice with the abnormalities seen in follistatin-overexpressing mice.

dnActRIB Blocks Activin Receptor-Mediated Signaling in Keratinocytes

Several findings suggest that activin receptor signaling is efficiently inhibited in keratinocytes of *K14-dnActRIB* transgenic mice: 1) we used a dominant-negative mutant, which had been well characterized in previous *in vitro* and *in vivo* studies and shown to inhibit activin but not TGF-β signaling;[17,32,33] 2) expression of the dominant-negative mutant was at least more than 10-fold higher compared to the endogenous receptor; 3) phosphorylation of Smad2 and its subsequent nuclear translocation were inhibited in cultured murine keratinocytes from *K14-dnActRIB* transgenic mice; and 4) the phenotype of activin-overexpressing mice was strongly reduced in mice double-transgenic for both activin βA and dnActRIB. Although activin and TGF-β use similar signaling pathways in keratinocytes, including phosphorylation of Smad2/Smad3,[16] the inhibitory effect of dnActRIB was specific for activin. Thus, signaling via the related TGF-β receptor complexes was not inhibited in cultured keratinocytes from *K14-dnActRIB* transgenic mice. Furthermore, mice expressing a dominant-negative TGF-β receptor mutant in the epidermis had a different wound-healing phenotype compared to *K14-dnActRIB* transgenic mice.[34] In conclusion, activin receptor signaling is suppressed in keratinocytes of *K14-dnActRIB* transgenic mice.

Keratinocytes Respond to Activin during Hair Follicle Morphogenesis

Consistent with the normal proliferation and differentiation of interfollicular keratinocytes seen in the skin of follistatin-overexpressing mice,[13] these processes were also unaltered in *K14-dnActRIB* transgenic animals. This finding further suggests that the low levels of activin present in normal adult skin do not affect epidermal homeostasis. By contrast, activin is expressed at higher levels in embryonic and newborn skin (S.W., unpublished data),[35] which may suggest a more important role of activin during skin development than in adult murine skin. Indeed, *K14-dnActRIB* transgenic mice displayed a discrete delay in the early stages of hair follicle morphogenesis, demonstrating that keratinocytes constitute an activin-responsive cell type during hair follicle morphogenesis, yet is not essential for hair development to occur. Likewise, activin receptor-mediated signaling also seems to be required for normal catagen-telogen transformation during the initiation of hair follicle cycling immediately after the completion of postnatal hair follicle morphogenesis in mice. Surprisingly, both follistatin knockout mice and activinβA-overexpressing mice also showed a significant retardation of hair follicle morphogenesis.[36] This finding suggests that the hyperactive activin in the follistatin knockout mice or the overexpressed activin exert an inhibitory effect on hair follicle morphogenesis via activation of stromal cells. Alternatively, the effect of activin on hair follicle morphogenesis may be dose-dependent. In this case the low levels of endogenous activin would be required for the progression of hair follicle morphogenesis, whereas elevated levels as seen in follistatin knockout mice or activin-overexpressing mice may have the opposite effect.

ActivinβA knockout mice show a complete absence of whisker hair follicles at birth.[10] This phenotype was not recapitulated in our *K14-dnActRIB* transgenic mice. This suggests that activin is only required at an earlier stage of development of vibrissae follicles, when the K14 promoter-driven dnActRIB transgene is not yet expressed at sufficiently high levels. This possibility is supported by the expression of activinβA in the mesenchyme of developing vibrissae at embryonic day 10.5,[37] a time point that precedes the onset of strong transgene expression. Alternatively, activin may exert its effect on whisker development predominantly via induction of proteins in stromal cells, which then act on keratinocytes in a paracrine manner.

Figure 6. Wound healing in *K14-dnActRIB* transgenic mice. **A:** H&E-stained sections of paraffin-embedded back skin wounds at days 3, 5, and 13 after injury, are shown. **Arrowheads** indicate the position of the tip of the hyperproliferative epithelium. **B:** Forty-μg samples of total cellular RNA from normal skin and skin wounds of different stages from wild-type and *K14-dnActRIB* transgenic mice were analyzed for the presence of activinβA mRNA by RPA. One μg of the RNAs was loaded on a 1.5% agarose gel and stained with ethidium bromide as a control (**bottom**). **C:** The bar graph shows the percentage of day 5 wounds, which were completely re-epithelialized in *K14-dnActRIB* transgenic and wild-type mice (**black bars**). Quantitative analysis of the wound-healing process: box plots show the results obtained for the number of $BrdU^+$ cells per area (10^3 μm^2) in the hyperproliferative epithelium (**D**), the absolute area of the hyperproliferative epithelium (**E**), and the length of the wound epidermis (**F**). Shown are median values, 25th to 75th percentile (**boxes**), and range (**vertical bars**). The number of wound halves (n) analyzed from a total number (N) of mice and the P value determined by the Students' t-test is indicated underneath each diagram ($^*P < 0.05$, $^{**}P < 0.01$, $^{***}P < 0.001$). D, dermis; dw, days wounded; ES, eschar; G, granulation tissue; HE, hyperproliferative epithelium. Scale bars, 100 μm (**A**).

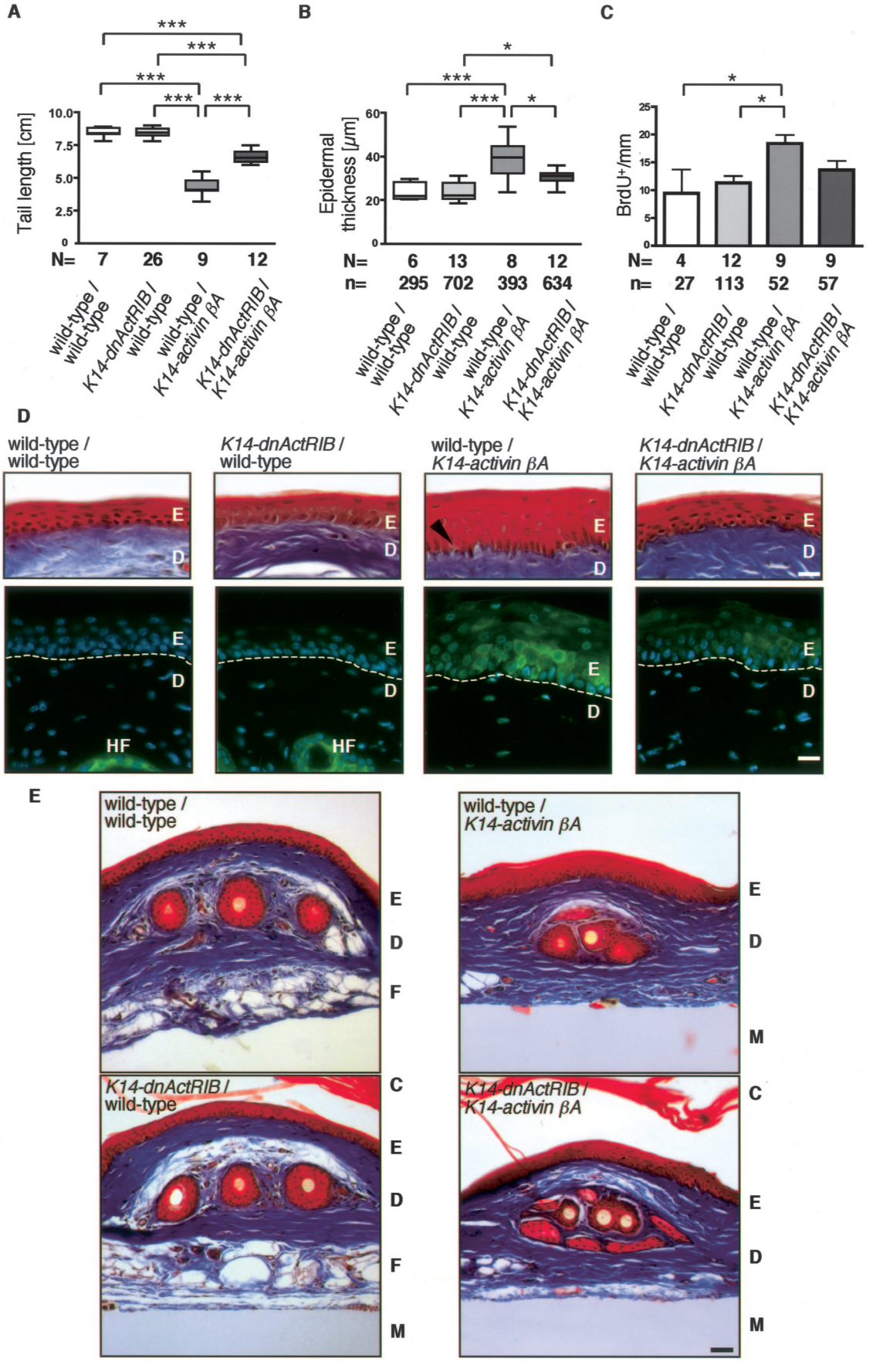
A
B
C
Tail length [cm]
Epidermal thickness [μm]
BrdU+/mm
N= 7 26 9 12
N= 6 13 8 12
n= 295 702 393 634
N= 4 12 9 9
n= 27 113 52 57
wild-type / wild-type
K14-dnActRIB / wild-type
wild-type / K14-activin βA
K14-dnActRIB / K14-activin βA
D
E
D
HF
E
F
M
C

Endogenous Activin Stimulates Wound Re-Epithelialization at Least in Part via Keratinocytes

In addition to the delay in pelage hair follicle morphogenesis, we also observed a slightly delayed wound re-epithelialization in *K14-dnActRIB* transgenic mice. This effect was not due to an altered proliferation rate or a premature onset of differentiation of wound keratinocytes. Furthermore, no difference in apoptosis was detected, indicating that the observed abnormalities might result from reduced keratinocyte motility in the absence of activin signaling. This hypothesis is supported by the reduced length of the migrating epithelial tongue in wounds of *K14-dnActRIB* transgenic mice. Thus, activin signaling in keratinocytes seems to promote motility of these cells in wounded skin. By contrast, preliminary scratch wounding experiments did not reveal a significant enhancement of keratinocyte migration by activin A *in vitro* (data not shown). This result further confirms that the effect of activin on keratinocytes is different *in vitro* and *in vivo* (see below).

Interestingly, the severe reduction in granulation tissue formation, which was seen in follistatin-overexpressing mice, was not recapitulated in *K14-dnActRIB* transgenic animals. This phenotype of the follistatin transgenic animals is not a result of inhibition of bone morphogenetic proteins by follistatin, because mice double-transgenic for activin and follistatin had normal wound healing (S.W., unpublished data).[13] Rather, these results as well as the data with *K14-dnActRIB* transgenic animals presented here suggest that activation of stromal cells in the wound by endogenous activin is required for normal granulation tissue formation and that activin receptor signaling in both keratinocytes and stromal cells is required for efficient repair of the dermis and epidermis.

Concentration-Dependent Modulation of the Epidermal Architecture by Activin

Because activin is known to act as a morphogen,[2] we wondered whether pathologically high levels of activin affect keratinocytes in normal and wounded skin. For this purpose, we determined if the epidermal hyperplasia seen in activin-overexpressing mice[12] can be rescued by breeding of the animals with *K14-dnActRIB* transgenic mice. Indeed, several characteristic abnormalities of the activin-overexpressing mice were at least partially reversed, including the short length of the tail, the epidermal hyperplasia and the abnormal keratinocyte organization, the hyperproliferation of these cells, as well as the interfollicular expression of keratin 6. Although we cannot fully exclude the possibility, that the high levels of dnActRIB sequester the epidermis-derived activin and thus prevent it from a paracrine activation of dermal cells, this seems unlikely, because the dnActRIB alone does not bind to activin,[32] and because the dermal phenotype was still present in *K14-dnActRIB/K14-activinβA* double-transgenic mice. Rather, our results suggest that high levels of activin affect keratinocyte proliferation and differentiation at least in part via direct activation of keratinocytes.

The Effect of Activin on Keratinocytes Is Different in Vitro *and* in Vivo

Surprisingly, however, activin appears to stimulate keratinocyte proliferation *in vivo*, whereas the opposite effect was observed *in vitro* (our own unpublished data).[16] Furthermore, the results presented in this study suggest that activin also affects keratinocyte migration in wounded skin, although we could not detect a promigratory effect of activin A for keratinocytes *in vitro* in preliminary experiments. A similar discrepancy between *in vivo* and *in vitro* results was also observed when latent TGF-β1 was constitutively overexpressed in keratinocytes at low levels.[38] However, activin overexpression in the epidermis did not induce an inflammatory response[12] as seen in the skin of latent TGF-β1-overexpressing mice.[38] Presumably, additional signals present in skin but not in cell culture, are necessary to transform the growth inhibitory effect of activin *in vitro* into a proliferation-stimulating effect in mouse skin *in vivo*. Likewise, activin-induced terminal differentiation as indicated by *in vitro* experiments[39] was not reflected by the phenotype of *K14-activinβA*-overexpressing mice nor did we observe obvious differentiation abnormalities in the epidermis of *K14-dnActRIB* transgenic mice. Therefore, it seems likely that one or more additional factors are present *in vivo* but not *in vitro*, which modulate the response of keratinocytes to activin. The latter may be produced by stromal cells and act in a paracrine manner on the epidermis. There are several examples of growth factors, which stimulate keratinocyte proliferation in a paracrine manner, eg, keratinocyte growth factor and granulocyte-macrophage colony stimulating factor.[40] The effect of such factors may be medi-

Figure 7. dnActRIB reduces the *K14-activinβA*-induced phenotype. **A:** The tail-length of wild-type mice and mice single or double transgenic for *K14-dnActRIB* and *K14-activinβA* was determined (N, number of mice investigated). **B:** The thickness of the epidermis was measured in orthokeratotic regions of the tail. The epidermal hyperthickening in activin-overexpressing mice is partially rescued by dnActRIB (N, number of mice; n, number of measurements performed in different areas of the tails). **C:** BrdU incorporation studies revealed the number of proliferating keratinocytes per mm of tail epidermis. Note the hyperproliferation of basal keratinocytes in activin-overexpressing mice and the almost complete rescue by dnActRIB. The significance was determined using the Bonferroni correction (**A–C**), eg, $*P < 0.05$ and $***P < 0.001$ (N, number of mice; n, number of measurements performed in different areas of the tails). The epidermis of Masson trichrome-stained tail skin from wild-type, single-transgenic, and double-transgenic mice is shown at high magnification in **D**. Note the enlarged spinous layer in *K14-activinβA* mice when compared to *K14-dnActRIB* transgenic or wild-type mice. The **arrow** points to densely packed keratinocytes in activin βA-overexpressing single-transgenic mice. Immunohistochemistry localized keratin 6 expression, visualized as Cy2 (green) fluorescence in keratinocytes of the interfollicular epidermis. Cell nuclei are stained with Hoechst 33258 (blue). The staining shows presence of keratin 6 in the epidermis of *K14-activinβA* transgenic mice, its reduced expression in *K14-dnActRIB/K14-activinβA* double-transgenic mice, and the lack of keratin 6 expression in interfollicular epidermis of wild-type and *K14-dnActRIB* transgenic mice. **Dotted line**: basal lamina. **E:** Sections from tail skin of wild-type, single- and double-transgenic mice were stained by Masson/Trichrome. Fatty tissue is replaced by connective tissue in both *K14-activinβA* and in *K14-dnActRIB/K14-activinβA* transgenic mice. Abbreviations: C, cornified layer; D, dermis; E, epidermis; F, fatty tissue; HF, hair follicle; M, nitrocellulose membrane. Scale bars: 50 μm (**D**); 10 μm (**E**).

ated at least in part via activin. Indeed, a recent example showed that activin is required for FGF-mediated effects on neurons,[41] and a similar FGF/activin interaction may occur in the skin. Alternatively, activin may also modulate wnt-mediated signals, since a recent study revealed that expression of TCF/LEF target genes can be controlled by wnt and TGF-β signaling in a cooperative manner.[42]

Taken together, the *K14-dnActRIB* transgenic mice revealed that endogenous activin affects hair follicle morphogenesis and wound re-epithelialization at least in part via activation of keratinocytes. By contrast, the positive effect of endogenous activin on granulation tissue formation during wound repair is mediated via the stroma. In addition, first wound-healing studies with *K14-dnActRIB/K14-activinβA* double-transgenic mice suggest that dnActRIB does not alter the activin-mediated enhancement of granulation tissue formation, indicating that this activity of the overexpressed activin is also mediated via stromal cells. Therefore, our results demonstrate that activin regulates skin morphogenesis and wound repair via keratinocytes and stromal cells in a concentration-dependent manner, and they highlight the importance of epithelial-mesenchymal interactions *in vivo*.

Acknowledgments

We thank C. Born-Berclaz for excellent technical assistance; Dr. D. Gospodarowicz, Chiron Corp., Emeryville, CA, for providing recombinant activin A; Dr. P. ten Dijke and Dr. C.-H. Heldin for the polyclonal antiserum directed against phosphorylated Smad2; Dr. P. Bugnon for help with the wound-healing experiments; and Dr. H. Kögel for invaluable help with the histomorphometry.

References

1. Lin SY, Morrison JR, Phillips DJ, de Kretser DM: Regulation of ovarian function by the TGF-beta superfamily and follistatin. Reproduction 2003, 126:133–148
2. Kerszberg M, Wolpert L: Mechanisms for positional signalling by morphogen transport: a theoretical study. J Theor Biol 1998, 191:103–114
3. Shimizu K, Gurdon JB: A quantitative analysis of signal transduction from activin receptor to nucleus and its relevance to morphogen gradient interpretation. Proc Natl Acad Sci USA 1999, 96:6791–6796
4. Dyson S, Gurdon JB: The interpretation of position in a morphogen gradient as revealed by occupancy of activin receptors. Cell 1998, 93:557–568
5. Phillips DJ: Regulation of activin's access to the cell: why is mother nature such a control freak? Bioessays 2000, 22:689–696
6. ten Dijke P, Hill CS: New insights into TGF-beta-Smad signalling. Trends Biochem Sci 2004, 29:265–273
7. Attisano L, Wrana JL, Montalvo E, Massague J: Activation of signalling by the activin receptor complex. Mol Cell Biol 1996, 16:1066–1073
8. Ten Dijke P, Goumans MJ, Itoh F, Itoh S: Regulation of cell proliferation by Smad proteins. J Cell Physiol 2002, 191:1–16
9. Nakamura T, Takio K, Eto Y, Shibai H, Titani K, Sugino H: Activin-binding protein from rat ovary is follistatin. Science 1990, 247:836–838
10. Matzuk MM, Kumar TR, Vassalli A, Bickenbach JR, Roop DR, Jaenisch R, Bradley A: Functional analysis of activins during mammalian development. Nature 1995, 374:354–356
11. Matzuk MM, Lu N, Vogel H, Sellheyer K, Roop DR, Bradley A: Multiple defects and perinatal death in mice deficient in follistatin. Nature 1995, 374:360–363
12. Munz B, Smola H, Engelhardt F, Bleuel K, Brauchle M, Lein I, Evans LW, Huylebroeck D, Balling R, Werner S: Overexpression of activin A in the skin of transgenic mice reveals new activities of activin in epidermal morphogenesis, dermal fibrosis and wound repair. EMBO J 1999, 18:5205–5215
13. Wankell M, Munz B, Hubner G, Hans W, Wolf E, Goppelt A, Werner S: Impaired wound healing in transgenic mice overexpressing the activin antagonist follistatin in the epidermis. EMBO J 2001, 20:5361–5372
14. Hübner G, Hu Q, Smola H, Werner S: Strong induction of activin expression after injury suggests an important role of activin in wound repair. Dev Biol 1996, 173:490–498
15. Cruise BA, Xu P, Hall AK: Wounds increase activin in skin and a vasoactive neuropeptide in sensory ganglia. Dev Biol 2004, 271:1–10
16. Shimizu A, Kato M, Nakao A, Imamura T, ten Dijke P, Heldin CH, Kawabata M, Shimada S, Miyazono K: Identification of receptors and Smad proteins involved in activin signalling in a human epidermal keratinocyte cell line. Genes Cells 1998, 3:125–134
17. Zhou Y, Sun H, Danila DC, Johnson SR, Sigai DP, Zhang X, Klibanski A: Truncated activin type I receptor Alk4 isoforms are dominant negative receptors inhibiting activin signaling. Mol Endocrinol 2000, 14:2066–2075
18. Reissmann E, Jornvall H, Blokzijl A, Andersson O, Chang C, Minchiotti G, Persico MG, Ibanez CF, Brivanlou AH: The orphan receptor ALK7 and the activin receptor ALK4 mediate signaling by nodal proteins during vertebrate development. Genes Dev 2001, 15:2010–2022
19. Tsuchida K, Vaughan JM, Wiater E, Gaddy-Kurten D, Vale WW: Inactivation of activin-dependent transcription by kinase-deficient activin receptors. Endocrinology 1995, 136:5493–5503
20. Werner S, Breeden M, Hubner G, Greenhalgh DG, Longaker MT: Induction of keratinocyte growth factor expression is reduced and delayed during wound healing in the genetically diabetic mouse. J Invest Dermatol 1994, 103:469–473
21. Yang H, Wanner IB, Roper SD, Chaudhari N: An optimized method for in situ hybridization with signal amplification that allows the detection of rare mRNAs. J Histochem Cytochem 1999, 47:431–446
22. Chomczynski P, Sacchi N: Single-step method of RNA isolation by acid guanidinium thiocyanate-phenol-chloroform extraction. Anal Biochem 1987, 162:156–159
23. Bamberger C, Pollet D, Schmale H: Retinoic acid inhibits downregulation of deltaNp63alpha expression during terminal differentiation of human primary keratinocytes. J Invest Dermatol 2002, 118:133–138
24. Caldelari R, Suter MM, Baumann D, De Bruin A, Muller E: Long-term culture of murine epidermal keratinocytes. J Invest Dermatol 2000, 114:1064–1065
25. Paus R, Muller-Rover S, Van Der Veen C, Maurer M, Eichmuller S, Ling G, Hofmann U, Foitzik K, Mecklenburg L, Handjiski B: A comprehensive guide for the recognition and classification of distinct stages of hair follicle morphogenesis. J Invest Dermatol 1999, 113:523–532
26. Muller-Rover S, Handjiski B, van der Veen C, Eichmuller S, Foitzik K, McKay IA, Stenn KS, Paus R: A comprehensive guide for the accurate classification of murine hair follicles in distinct hair cycle stages. J Invest Dermatol 2001, 117:3–15
27. Magerl M, Tobin DJ, Muller-Rover S, Hagen E, Lindner G, McKay IA, Paus R: Patterns of proliferation and apoptosis during murine hair follicle morphogenesis. J Invest Dermatol 2001, 116:947–955
28. Schmidt-Ullrich R, Paus R: Molecular principles of hair follicle induction and morphogenesis. BioEssays 2005, 27:247–261
29. Stenn KS, Paus R: Controls of hair follicle cycling. Physiol Rev 2001, 81:449–494
30. Paus R, Foitzik K: In search of the "hair cycle clock": a guided tour. Differentiation 2004, 72:489–511
31. Sulyok S, Wankell M, Alzheimer C, Werner S: Activin: an important regulator of wound repair, fibrosis, and neuroprotection. Mol Cell Endocrinol 2004, 225:127–132
32. Harrison CA, Gray PC, Koerber SC, Fischer W, Vale W: Identification of a functional binding site for activin on the type I receptor ALK4. J Biol Chem 2003, 278:21129–21135
33. Chen Y, Mironova E, Whitaker LL, Edwards L, Yost HJ, Ramsdell AF: ALK4 functions as a receptor for multiple TGF beta-related ligands to

regulate left-right axis determination and mesoderm induction in Xenopus. Dev Biol 2004, 268:280–294
34. Amendt C, Mann A, Schirmacher P, Blessing M: Resistance of keratinocytes to TGFbeta-mediated growth restriction and apoptosis induction accelerates re-epithelialization in skin wounds. J Cell Sci 2002, 115:2189–2198
35. Munz B, Hubner G, Tretter Y, Alzheimer C, Werner S: A novel role of activin in inflammation and repair. J Endocrinol 1999, 161:187–193
36. Nakamura M, Matzuk MM, Gerstmayer B, Bosio A, Lauster R, Miyachi Y, Werner S, Paus R: Control of pelage hair follicle development and cycling by complex interactions between follistatin and activin. FASEB J 2003, 17:497–499
37. Feijen A, Goumans MJ, van den Eijnden-van Raaij AJ: Expression of activin subunits, activin receptors and follistatin in postimplantation mouse embryos suggests specific developmental functions for different activins. Development 1994, 120:3621–3637
38. Li AG, Wang D, Feng XH, Wang XJ: Latent TGFbeta1 overexpression in keratinocytes results in a severe psoriasis-like skin disorder. EMBO J 2004, 23:1770–1781
39. Seishima M, Nojiri M, Esaki C, Yoneda K, Eto Y, Kitajima Y: Activin A induces terminal differentiation of cultured human keratinocytes. J Invest Dermatol 1999, 112:432–436
40. Werner S, Smola H: Paracrine regulation of keratinocyte proliferation and differentiation. Trends Cell Biol 2001, 11:143–146
41. Tretter YP, Hertel M, Munz B, ten Bruggencate G, Werner S, Alzheimer C: Induction of activin A is essential for the neuroprotective action of basic fibroblast growth factor in vivo. Nat Med 2000, 6:812–815
42. Attisano L, Labbe E: TGFbeta and Wnt pathway cross-talk. Cancer Metastasis Rev 2004, 23:53–61